Human Molecular Genetics, 2009, Vol. 18, No. 8 **1384–1394**
doi:10.1093/hmg/ddp044
Advance Access published on January 24, 2009

Gigaxonin controls vimentin organization through a tubulin chaperone-independent pathway

Don W. Cleveland[1], Koji Yamanaka[1,2,3] and Pascale Bomont[1,4,5,*]

[1]Ludwig Institute for Cancer Research, Department of Cellular and Molecular Medicine, University of California at San Diego, La Jolla, CA 92093, USA, [2]Yamanaka Research Unit, RIKEN Brain Science Institute, Wako, Saitama 351-0198, Japan, [3]CREST, Japan Science and Technology Agency, Japan, [4]INSERM, U901, INMED, Marseille 13009, France and [5]Aix Marseille Université, Faculté des Sciences, Marseille F-13000, France

Received December 18, 2008; Revised and Accepted January 21, 2009

Gigaxonin mutations cause the fatal human neurodegenerative disorder giant axonal neuropathy (GAN). Broad deterioration of the nervous system in GAN patients is accompanied by massive disorganization of intermediate filaments (IFs) both in neurons and many non-neuronal cells. With newly developed antibodies, gigaxonin is now shown to be expressed at extremely low levels throughout the nervous system. In lymphoblast cell lines derived from severe and mild forms of GAN, mutations in gigaxonin are shown to yield highly unstable proteins, thereby permitting a rapid diagnostic test for the spectrum of GAN mutations as an alternative to invasive nerve biopsy or systematic sequencing of the *GAN* gene. Gigaxonin has been proposed as a substrate adaptor for an E3 ubiquitin ligase, which affects proteasome-dependent degradation of microtubule-related proteins including MAP1B, MAP8 and the tubulin folding chaperone TBCB. We demonstrate that, unlike its counterpart TBCE, TBCB only moderately destabilizes microtubules. Neither TBCB abundance nor microtubule organization or densities are altered in GAN mutant fibroblasts, thus demonstrating that altered TBCB levels are not primary determinants of IF disorganization in GAN. Characteristic GAN mutant-induced ovoid aggregates of vimentin are not produced in normal fibroblasts after disrupting microtubule assembly, either by TBCE overexpression or depolymerizing drugs. Thus, IF disorganization in GAN fibroblasts is independent of TBCB and microtubule loss and must be regulated by a yet unidentified mechanism.

INTRODUCTION

Giant axonal neuropathy (GAN; OMIM 256850) is an early onset progressive neurodegenerative disorder fatal in the young adult (1–3). GAN is caused by recessively inherited mutations in the *GAN* gene encoding the 65 kDa protein gigaxonin (4), a member of the BTB–Kelch family. The broad degradation of motor and sensory functions in the peripheral nervous system beginning early in infancy and later also impairing the central nervous system (including mental retardation, ataxia, nystagmus) (1,3,5,6) support an essential role of the *GAN* gene in neuronal maintenance. Examination of peripheral nerve biopsies has revealed a diminution of the density of nerve fibers (1,3). Concomitant with axonal loss, highly enlarged axons with an abnormally thin myelin sheath have been detected both in peripheral nerve and in the brain (1,3,7,8). Although the relevance of these so-called giant axons to the progression of disease and the degenerating process has not been established, their presence in nerve biopsies has long been considered sufficient to diagnose GAN. Nevertheless, the recent detection of similar giant axons in different forms of the inherited motor and sensory neuropathy Charcot–Marie–Tooth disease (9–12) showed that enlarged axons are not uniquely formed in GAN, therefore reinforcing the need for the development of a more specific diagnostic tool.

Although abnormal accumulation of neurofilaments (NFs) is detected in many human neurodegenerative disorders including amyotrophic lateral sclerosis (ALS), Parkinson's disease and Charcot–Marie–Tooth disease (13), a defining characteristic of GAN is that all intermediate filament (IF) types investigated

*To whom correspondence should be addressed at: INMED-INSERM U901, Parc scientifique de Luminy, 163 route de Luminy, BP13, 13273 Marseille Cedex 09, France. Tel: +33 4 91 82 81 00; Fax: +33 4 91 82 81 01; Email: pbom@inmed.univ-mrs.fr

© *The Author 2009. Published by Oxford University Press. All rights reserved.*
For Permissions, please email: journals.permissions@oxfordjournals.org

are abnormally organized both in neurons and non-neuronal cells (1,3,14,15). This includes abnormal aggregation of NFs in giant axons, desmin in muscles fibers, GFAP in astrocytes, keratin in hair and vimentin in multiple cell types including primary fibroblasts derived from skin biopsies of GAN patients. For example, we and others have used such primary cells to show that vimentin filament aggregation, whose frequency increases upon prolonged serum deprivation and confluence, is not associated with noticeable alteration of the actin filaments or the microtubule network (14,16–18). The extensive alteration of IF distribution in GAN patients suggests a very critical and direct role of gigaxonin in IF organization by a mechanism that still remains to be identified.

Despite its rare prevalence (4,19–26), attention on GAN has become increasingly more pronounced since the identification of gigaxonin as a key player in the ubiquitin proteasome system (UPS). This protein quality control targets unwanted or damaged proteins for degradation by the proteasome through the addition of an ubiquitin chain, a catalytic process performed by three enzymes E1 (ubiquitin-activating enzyme), E2 (ubiquitin-conjugating enzyme) and E3 (ubiquitin protein ligase). Although this crucial UPS protein quality control has been shown to be impaired in many neurodegenerative disorders, including ALS, Alzheimer's and Parkinson's diseases (27), the identification of gigaxonin in GAN (4) and parkin in autosomal recessive juvenile parkinsonism (28), as E3 ligases (or as substrate adaptor for such ligases), has focused attention on errors in this pathway in directly causing neurodegenerative diseases. For gigaxonin, as a proposed substrate adaptor of a Cul3-dependant E3 ubiquitin ligase (29–31), it apparently confers substrate specificity through direct interaction of substrates with its C-terminal Kelch domain. Accordingly, the abundance of three proposed partners of gigaxonin, the microtubule-associated proteins MAP1B (32), MAP8 (33) and the tubulin chaperone TBCB (34) has been shown to be altered *in vitro* through their interaction with gigaxonin, with levels of all three also reported to be increased in tissues from mice deleted in exons 3–5 of the *GAN* gene ($GAN^{\Delta 3-5;\ \Delta 3-5}$) (32–34).

A mutation-mediated reduction in the activity of gigaxonin acting on these proposed partners would be expected to have opposing effects on microtubule networks: MAP1B is a microtubule stabilizing factor (35), whereas high levels of TBCB destabilize them (36). In human, and mouse as recently reported in a second GAN mouse model ($GAN^{\Delta 1;\Delta 1}$) (37), however, there is a widespread aberrant accumulation of IFs, raising the possibility that such aggregation results from a microtubule reorganization/destabilization. The interactions between IFs, and in particular vimentin, and microtubules have been demonstrated many times, including the coalignment of vimentin with subpopulation of microtubules and the reorganization of vimentin network in response to microtubule damage (as a result of microtubule depolymerizating drugs and microinjection of specific antibodies against IFs, microtubules and their associated proteins) (38–44).

Using primary fibroblasts derived from skin biopsies of GAN patients in which aberrant ovoids of vimentin filaments are accumulated, we now determine that gigaxonin mutations do not affect microtubule density or TBCB levels. Moreover, GAN-like aggregates of vimentin are not induced in normal fibroblasts even after prolonged depletion of microtubule arrays. Altogether, not only is TBCB not a potent destabilizer of microtubules, the generalized disorganization of IFs in GAN is not caused by microtubule loss or TBCB overabundance; rather, gigaxonin controls IF architecture by a yet unknown mechanism. Moreover, with newly generated monoclonal antibodies directed against two distinct epitopes of gigaxonin and lymphoblast cell lines from patients, we show that the gigaxonin E3 ligase subunit is normally expressed at a very low level and that various missense and nonsense mutations scattered across the entire *GAN* gene produce highly unstable protein products. Since gigaxonin is indistinguishably destabilized in patients with severe or milder forms of the disease, the measurement of gigaxonin levels in patient lymphoblasts provides a rapid and specific diagnostic test for GAN.

RESULTS

Gigaxonin is an ubiquitous low abundance protein

Using both an N-terminal portion and full-length gigaxonin as antigens, two monoclonal antibodies, GigA and GigB, were produced which bound human gigaxonin (Fig. 1A). Both recognized the 60 kDa endogenous gigaxonin in human and mouse brain extracts (Fig. 1B). The GigA and GigB epitopes were determined to be located within the BTB domain and the first-half of the Kelch domain, respectively, as revealed by their exclusive detection of N-terminal (224 amino acids) or C-terminal (456 amino acids) parts of gigaxonin (Fig. 1A and C). The epitope recognized by GigB was further mapped to lie between amino acid 224 and the cysteine at 393, because it was capable of detecting the truncated Gig^{C393X} mutant in a lymphoblast cell line derived from a GAN patient (Fig. 3B).

Immunoblotting with the GigA antibody and a standard curve generated from known amounts of the recombinant gigaxonin amino terminus (Gig^{1-224}) were used to determine that gigaxonin was expressed throughout the central and peripheral nervous system at very low levels. Indeed, in both it accounted for only 1.25×10^{-3} % of the proteins in detergent soluble lysates of mouse brain and human lymphoblasts. Similar evaluation of normal human lymphoblast lines revealed 7500 molecules per cell (Fig. 2).

A new specific diagnostic test for GAN

Expression levels of gigaxonin were determined in eight lymphoblast cells lines (L1–L8) derived from different GAN patients. Two of these (L2 and L7) came from patients with mild forms of the disease for which we previously identified the corresponding mutations (GAN^{R15S} and GAN^{R138H}) (4,19) (Fig. 3A). Except for undetermined mutations in one of the two alleles in three patients (who carry identified mutant GAN alleles GAN^{S79L} in patients L5 and L6 and mutant GAN^{V82F} in patient L3), all of the mutant proteins from the remaining alleles would be predicted to be recognized by both the GigA and GigB antibodies (including the nonsense mutations GAN^{C393X} and GAN^{R477X} which lie 3′ to the sequences encoding both epitopes). Regardless of the

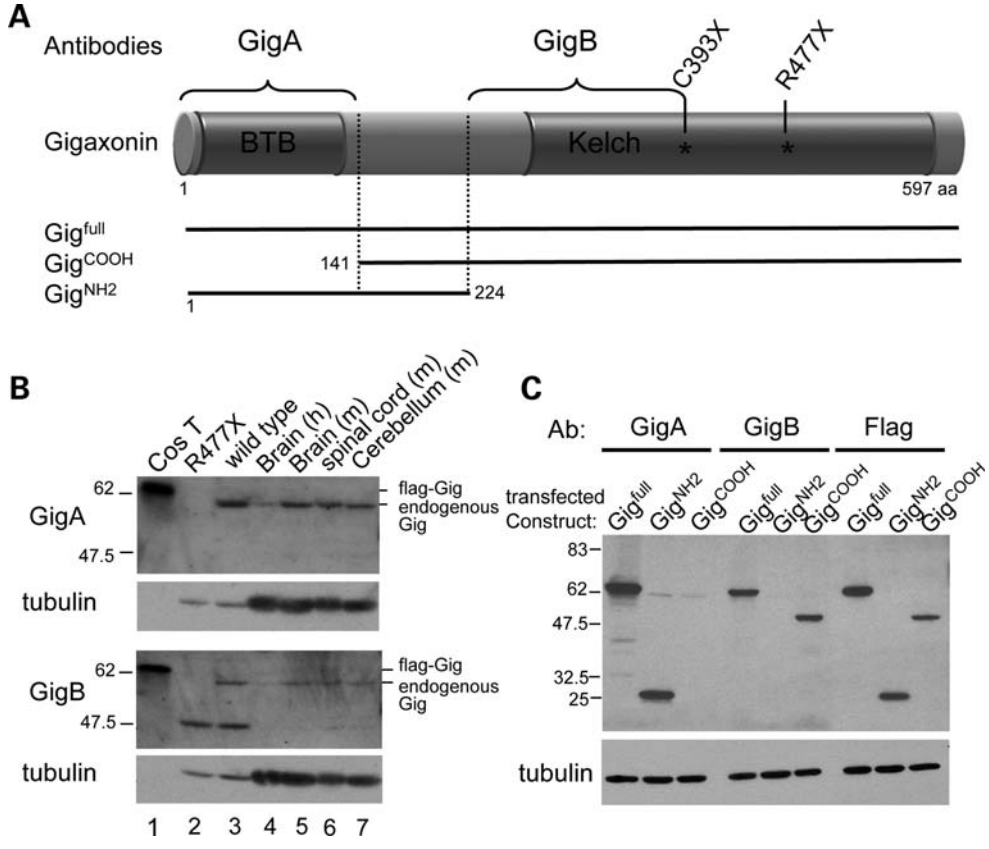

Figure 1. Generation of two monoclonal antibodies specific for gigaxonin. (**A**) Schematic representation of GigA and GigB epitopes. GigA and GigB monoclonal antibodies were generated using Gig^{NH2} and full-length gigaxonin as immunogens, respectively. (**B**) Specificity of GigA and GigB antibodies determined by immmunoblotting of extracts derived from (lane 1) Cos cells transfected to express flag-tagged full-length gigaxonin, (lanes 2 and 3) lymphoblasts derived from a GAN patient carrying a homozygous R477X mutation and control lymphoblast, respectively. Endogenous gigaxonin is detected in human brain (lane 4) and in mouse brain, spinal cord, cerebellum (lanes 5–7). (**C**) Immunoblot detection of gigaxonin by both gigaxonin antibodies using Cos cell extracts transfected with different gigaxonin constructions. Detection of Gig^{C393X} with the GigB antibody (in Fig. 3B) defines the GigB epitope to lie within the beginning of the Kelch domain.

type of mutation, the position on the *GAN* cDNA or the severity of the disease, mutant gigaxonin was found to be highly unstable, yielding an accumulated level barely detectable and at least 12-fold below that of wild-type gigaxonin (Fig. 3B, mutant gigaxonin correspond in average to $8 \pm 5.3\%$ of wild-type gigaxonin expression). This analysis of various known gigaxonin mutations confirms that there is a loss in the amount of this E3 ligase subunit in GAN, as expected for the recessive inheritance of disease. Furthermore, the substantial reduction seen not just for severe disease forms, but for milder ones as well, supports the use of this immunodetection method as a rapid diagnostic test, as an easier, less-invasive alternative to nerve biopsy examination or the very tedious screening of all 11 exons of the *GAN* gene for mutation analysis.

TBCB is not as potent as TBCE in depolymerizing microtubules

To test whether the tubulin chaperone TBCB, whose level has been proposed to be regulated by gigaxonin and to induce destabilization of microtubules (34), could affect IFs organization, both Cos cells and human primary fibroblasts derived from control skin biopsies were transfected in parallel with a pair of constructs encoding either the TBCB or TBCE components of the tubulin protein folding pathway (Fig. 4A) (45,46). The efficiency of each in destabilizing endogenous microtubules and any subsequent affect on vimentin organization was then determined by indirect immunofluorescence.

In almost all transfected Cos cells, forced expression of TBCE was sufficient to completely depolymerize the entire interphase microtubule array by 48 h post-transfection (Fig. 4B and C) (as previously described by others 45). TBCB, on the other hand, was much less efficient (Fig. 4B and C), with $64 \pm 4\%$ of TBCB transfected cells still retaining an intact microtubule network, with the remaining presenting, at best, only a slight reduction in microtubule intensity (asterisked starred in Fig. 4B). Vimentin organization was not noticeably affected by microtubule loss. Similar results were also obtained using HeLa cells (data not shown).

To address whether TBCB acts on the level of free tubulin dimers in addition to any affect on the array of microtubules, microtubules were quantitatively disassembled by treating cell cultures with nocodazole prior to fixation and visualization. Although unassembled tubulin was easily detected in wild-type cells after nocodazole treatment as expected, ectopic

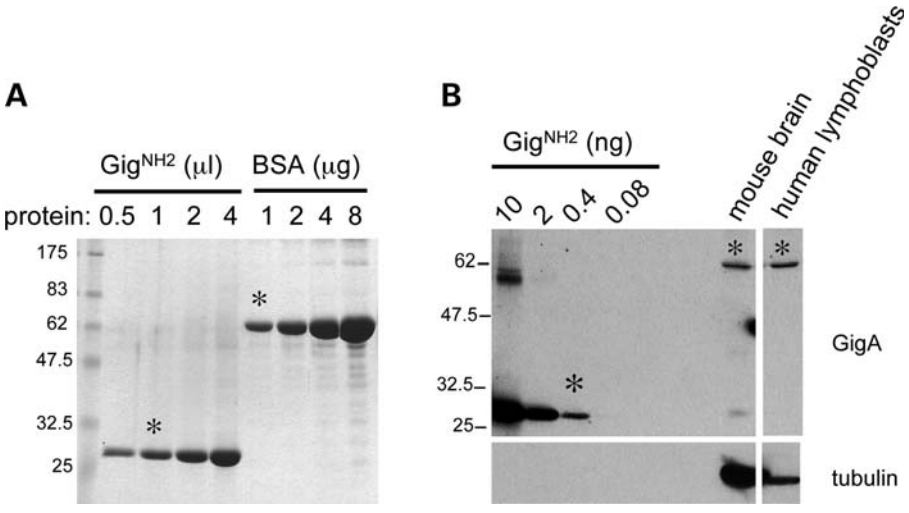

Figure 2. Gigaxonin is a low abundance protein. (**A**) Determination of the concentration of Gig^{NH2} recombinant gigaxonin by Coomassie blue staining of SDS gels and comparison with a dilution series of known amounts of bovine albumin. As shown by the stars, Gig^{NH2} is estimated to 1 μg/μl. (**B**) Abundance of endogenous gigaxonin was estimated using the GigA antibody and immunoblotting of brain or lymphoblast extracts and known amounts of purified Gig^{NH2}. Endogenous gigaxonin was calculated to represent 1.25×10^{-3}% of detergent soluble mouse brain lysate (i.e. 0.4 ng of the 234 amino acid Gig^{NH2} is found in 80 μg of mouse brain extract; this corresponds to $597/234 \times 0.4 = 1$ ng of full-length gigaxonin; 1 ng/80 μg $= 1.25 \times 10^{-3}$%). Gigaxonin is estimated at 7500 molecules per human lymphoblast cell [0.4 ng of Gig^{NH2} (corresponding to 1 ng of full-length gigaxonin) is present in extract from 2×10^5 lymphoblast cells; this is 5×10^{-15} g of gigaxonin per cell; at a molecular weight of 67×10^3; this corresponds to 7500 molecules per cell).

expression of TBCE eliminated detectable tubulin, consistent with its known role in tubulin folding and recycling (Fig. 4D and E). Parallel assessment following comparable expression of TBCB, on the other hand, left free tubulin levels detectable in more than 85% of cells (Fig. 4D and E), consistent with TBCB playing a less important role in maintaining tubulin levels than TBCE.

Considering the proposed role of gigaxonin in regulating TBCB levels *in vitro* (34), we addressed whether reintroduction of wild-type gigaxonin or disease-associated mutants could rescue the TBCB-mediated microtubule instability. To test this, wild-type or GAN-linked mutant genes were co-expressed along with TBCB in Cos cells. Analysis of the resultant cells revealed that wild-type gigaxonin, but none of the GAN-linked mutants, could partially protect against TBCB-mediated microtubule instability (Fig. 4F). On the other hand, gigaxonin had no effect on microtubule disassembly mediated by TBCE (Fig. 4F, bottom).

Neither TBCB abundance nor microtubule density is substantially altered in GAN primary fibroblasts

Although no obvious rearrangement of vimentin was found after elevation of TBCB in immortalized cell lines (Fig. 4B), we tested whether IF aggregation in GAN primary fibroblasts could be attributed to either TBCB overabundance and/or decreased microtubule density. While in control fibroblasts vimentin is assembled and organized into a homogeneously distributed array, a proportion of GAN cells carry aggregates of vimentin whose frequency increases after serum deprivation (Fig. 5A, right). We have previously shown that regardless of the type of *GAN* mutation, in normal growth conditions, 3–15% of the cells present such aggregates and the proportion markedly escalates (to 48–88%) upon serum starvation (14). (Exceptions to this are fibroblasts carrying the R15S mutation, for which vimentin aggregates are rarely seen in either serum condition.) Careful examination of two independent control fibroblasts and four unrelated GAN cell fibroblasts of known mutations (GAN^{R15S}, GAN^{R545C}, GAN^{R293X} and GAN^{R477X}) neither revealed serum conditions significantly altered microtubule distribution nor produced noticeable change in microtubule intensity (Fig. 5A, right). Furthermore, immunoblotting to determine endogenous TBCB levels, measured after prolonged serum starvation to enhance vimentin bundling, revealed no significant increase of TBCB in patient fibroblasts (Fig. 5B), including no difference between fibroblasts that develop vimentin bundles and the R15S fibroblasts with no vimentin aggregation.

Microtubule disassembly does not generate GAN-like vimentin aggregates

Although we neither detected an increase in TBCB level nor an obvious affect on assembled microtubule networks as a consequence of loss of gigaxonin in fibroblasts that might be central to the collapse of vimentin filaments into ovoid rings, we tested whether such ovoids could be produced by reducing microtubule content. For this, we forced prolonged microtubule disassembly in normal primary fibroblasts by two ways: addition of nocodazole to block new microtubule assembly and by overexpression of TBCE (Fig. 6). For the first approach, nocodazole was added and the consequences on microtubule and vimentin filaments were followed over a 72 h period. The resulting effect on vimentin organization was then assessed in interphase cells, exploiting that cell cycle timing in primary human fibroblasts ranges from 3 to 7 days. Vimentin was reorganized from an elongated network of fibers to a more relaxed and curved network that

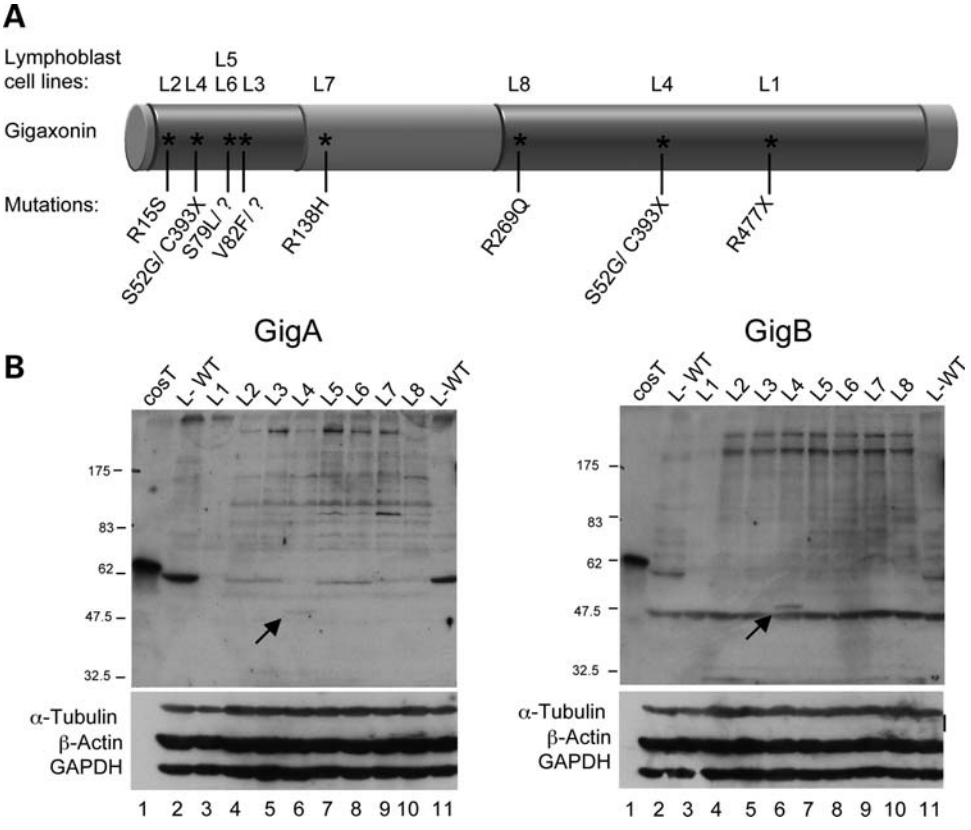

Figure 3. A new molecular diagnostic test for GAN. (**A**) Human lymphoblast cell lines (L1–L8) carrying different *GAN* mutations were expanded and harvested to produce cell extracts. L2 and L7 were derived from mildly affected patients. (**B**) Immunoblots of extracts of Cos cells transfected to express flag-tagged full-length gigaxonin (lane 1), a control human lymphoblast line (lanes 2 and 11), and GAN mutant cells L1–L8 (lanes 3–10). (Left) GigA antibody; (right) GigB antibody. Below are the same samples probed with tubulin, actin and GAPDH antibodies to serve as loading controls.

filled the entire cytoplasm as early as microtubule depolymerization was complete (within 3 h after nocodazole addition) and persisted over the 72 h period (Fig. 6A, left panel). This rearrangement was distinct from the ovoid aggregate of vimentin present in GAN fibroblasts grown in normal serum concentration and from the ovoid and ring aggregates that appear after prolonged culture in low serum (Fig. 6A, right panel). Nocodazole-induced depolymerization of microtubules leads to a dramatic collapse of the entire vimentin array in all GAN fibroblasts, demonstrating that a relatively intact array of microtubules is required to prevent such rearrangement.

The effect of microtubule destabilization on vimentin organization was also examined after increasing TBCE or TBCB levels for 72 h (Fig. 6B). Increased levels of TBCE induced a total depolymerization of microtubules (Fig. 6B left panel), whereas corresponding expression of TBCB only reduced microtubule density in a proportion of transfected cells (Fig. 6B, right panel). No effect on vimentin filament networks was detectable, and vimentin aggregates were never observed in cells with reduced microtubule content.

DISCUSSION

By generating two new distinct monoclonal antibodies GigA and GigB against the BTB and Kelch domains of gigaxonin, respectively, we have established that the 60 kDa migrating gigaxonin polypeptide accumulates to a very low level throughout the nervous system (only 1.25×10^{-3}% of detergent soluble brain lysate) and to only ~7500 molecules per cell in blood-derived lymphoblast cell lines. Our evidence demonstrates that unlike previously described gigaxonin antibodies, including one that identified a polypeptide at ~82 kDa (35) that cannot be authentic gigaxonin and another without control for specificity (47), our monoclonal antibodies detect exclusively endogenous gigaxonin in human lymphoblast cell lines. This is particularly important to develop a diagnostic test for GAN, since it offers a tool that allows for the detection of all pathogenic gigaxonin products, with the exception of truncated mutants located upstream of the GigA epitope within the BTB domain. Furthermore, using lymphoblasts cell lines from a series of *GAN* mutations, our efforts unambiguously demonstrate that regardless of the type of mutation and of the severity of the disease, pathogenic gigaxonin is highly unstable. We propose that an immunodetection method such as that we present here represents a rapid molecular test that can replace the current method of nerve biopsy, which apart from its invasive nature is now recognized not to provide an exclusive diagnosis of GAN, as the presence of giant axons is also found in the inherited motor and sensory neuropathy Charcot–Marie–Tooth disease (9–12). Furthermore, this simple immunological approach provides a rapid

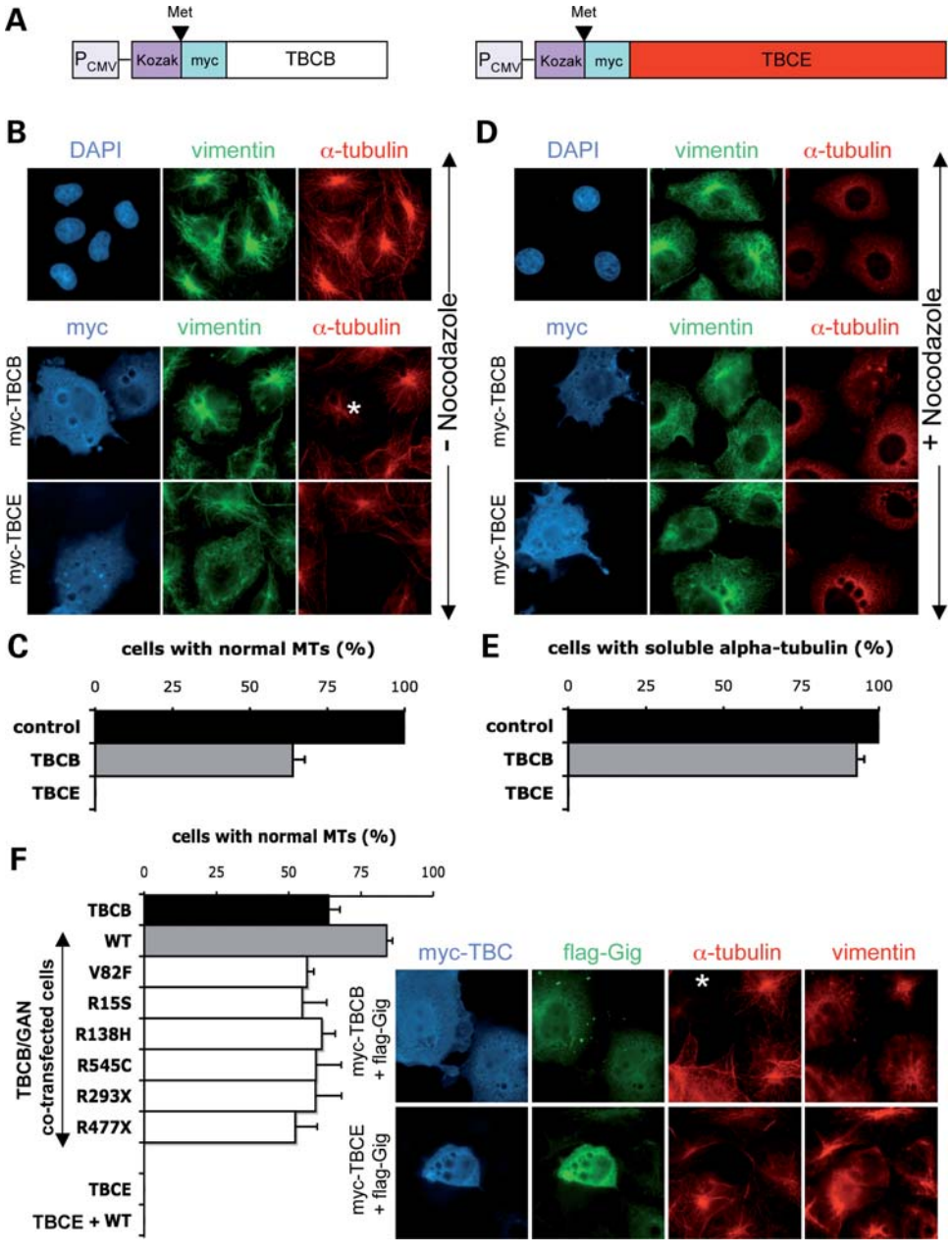

Figure 4. TBCE, but not TBCB, is a potent destabilizing agent of microtubules. The effects of increased synthesis of TBCB and TBCE on microtubule were assessed in Cos cells 48 h after transfection with (**A**) myc-TBCB or myc-TBCE constructs (**B**) in normal media and (**D**) after addition of 10 μM nocadozole for 1.5 h prior to fixation to convert the assembled tubulin pool to tubulin dimers. (The star in B shows a TBCB expressing cell with only a reduced density of microtubules.) (**C** and **E**) Quantification of experiments in (B) and (D) by analysis of 30–40 transfected cells in two independent experiments with and without nocodazole. (**F**) Myc-tagged TBCB or TBCE and flag-tagged wild-type gigaxonin or mutant gigaxonin were transfected into Cos cells, and microtubules assembly was assayed 48 h later (the star represents a TBCB-gigaxonin positive cell with no rescue).

alternative to the tedious screening for mutations within the 11 exons that constitute the *GAN* gene.

The recent proposal for gigaxonin as a substrate adaptor of a new Cul3-dependent E3 ubiquitin ligase (29–31) has fueled a novel possibility for the mechanism(s) by which this protein controls both neuronal integrity and IFs architecture and that when diminished in abundance leads to the devastating neurodegenerative disorder GAN in human. To date, three partners of gigaxonin have been proposed: the microtubule-associated protein MAP1B (32), MAP8 (33) and the tubulin cofactor TBCB (34). These partners offer a paradoxical view on any mechanism related to microtubule properties: absence of gigaxonin would presumably promote increases in the levels of all three partners, one of which (MAP1B) would stabilize microtubule network, but the last (TBCB) would destabilize tubulin and assembled microtubules. The abundance of each has been reported *in vitro* to be regulated by the proteasome through their interaction with gigaxonin and increased in

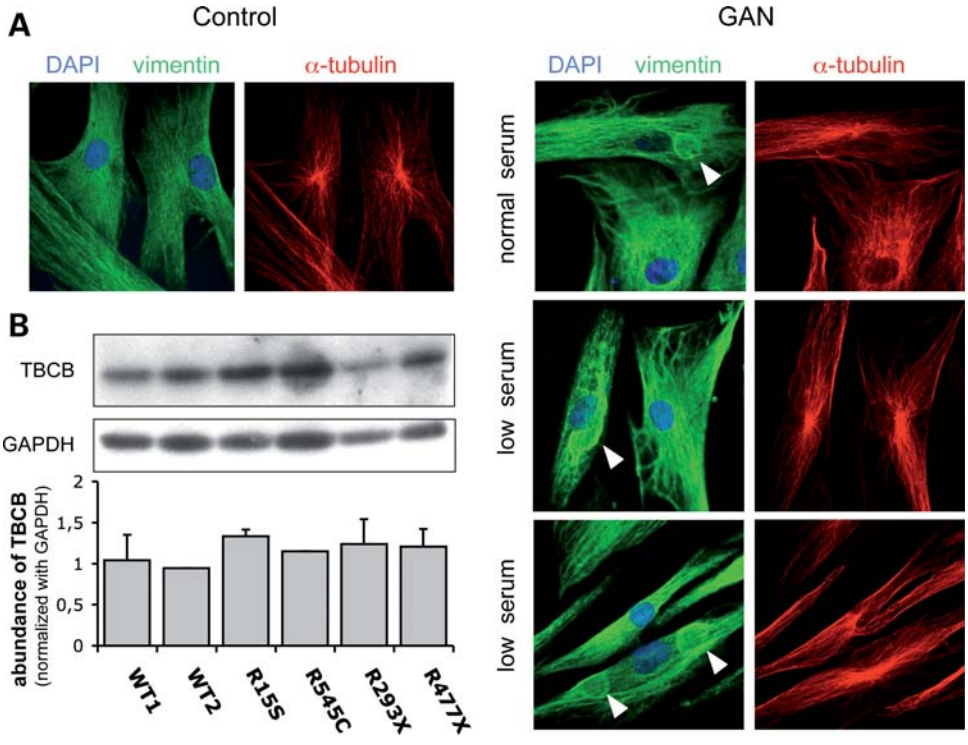

Figure 5. Neither MTs nor TBCB are noticeably altered in primary fibroblasts derived from GAN patients. (**A**) Microtubule overall distribution and density were compared between (left panel) two control fibroblasts and (right) four unrelated GAN patients fibroblasts (GAN^{R545C}, GAN^{R15S}, GAN^{R293X} and GAN^{R477X}) by immunofluorescence, in normal or low serum condition. Arrowheads represent the aggregates of vimentin in patient cells. (**B**) Endogenous abundance of TBCB was quantified by immunoblotting on control and unrelated GAN fibroblasts. This was measured in two independent extracts prepared from cultures in low serum to enhance vimentin bundling: 57 ± 7.6% for GAN^{R545C}; 0 ± 0% for GAN^{R15S}; 68.7 ± 15.3% for GAN^{R293X} and 66.8 ± 8.2% for GAN^{R477X} (14).

tissues from a mouse with a gene disruption in the *GAN* gene ($GAN^{\Delta 3-5;\Delta 3-5}$) (32–34). Moreover, an initial analysis of this first $GAN^{\Delta 3-5;\Delta 3-5}$ mouse reported a progressive reduction in spontaneous movement, ataxic gait and abnormal accumulation of NFs without formation of giant axons (33). The neurodegeneration engaged in GAN has been subsequently quantified in a second mouse model ($GAN^{\Delta 1;\ \Delta 1}$) to reveal an early aggregation of various IF types throughout the central and peripheral nervous system, followed at 6 months of age by hind limb muscle atrophy associated with a 10% decrease in muscle innervation and a 27% loss of motor axons (37).

The diminution of microtubule density in the first described GAN mouse model has been suggested to be attributed to TBCB overabundance (34). Indeed, these $GAN^{\Delta 3-5;\Delta 3-5}$ mice were reported to have reduced microtubule content in cortical neuron cultures and a corresponding decrease in microtubule density in tissues (34). The proposed alteration of microtubules in the initial $GAN^{\Delta 3-5;\Delta 3-5}$ mouse is at odds with the situation reported in humans, where the microtubule network is not noticeably altered in GAN primary fibroblasts (14,16,18) and has been shown in patient's nerves to be either mostly excluded from densely packed NFs regions thereby forming microtubule-enriched areas or even dramatically increased in axonal regions deprived of NFs (48,49).

A crucial, unsolved issue in GAN concerns how loss of gigaxonin affects IF organization inside and outside the nervous system—from neurons to hair. In this sense, GAN is distinguished from other neurodegenerative disorders that are accompanied by disorganization of NFs, without an effect on other classes of IFs. All of this suggests a central role of gigaxonin in maintaining IF integrity. Despite this, gigaxonin's proposed partners are not directly related to IFs, but are involved in tubulin synthesis/homeostasis and microtubule dynamics. In particular, the tubulin cofactor TBCB participates together with the other cofactors TBCA/C/D/E in tubulin biogenesis (46,50). Considering that upon overexpression, the cofactors TBCD/E/E-like, but not TBCC, have been shown to destabilize the microtubule network (45,51,52) (which we have confirmed here for TBCE, but with a much more modest effect for TBCB), it has been postulated that increased TBCB abundance, as reported in the $GAN^{\Delta 3-5;\ \Delta 3-5}$ deletion mice (34), could impair the corresponding microtubule stability.

Our evidence makes the proposal of microtubule instability from elevated TBCB in the absence of gigaxonin, an unlikely explanation for gigaxonin's effect on IF arrays, especially outside the nervous system including vimentin arrays in fibroblasts. We have found here that TBCB does not efficiently alter microtubule disassembly nor soluble tubulin subunit pool, in agreement with a recent study (36). Furthermore, neither endogenous TBCB nor microtubule density in fibroblasts carrying several *GAN* mutations differ noticeably from those found in normal fibroblasts. Considering that in patients' nerves, microtubules are present but excluded from densely packed NFs and even increased in axons deprived of NFs (48,49); the decrease of microtubule density reported in the

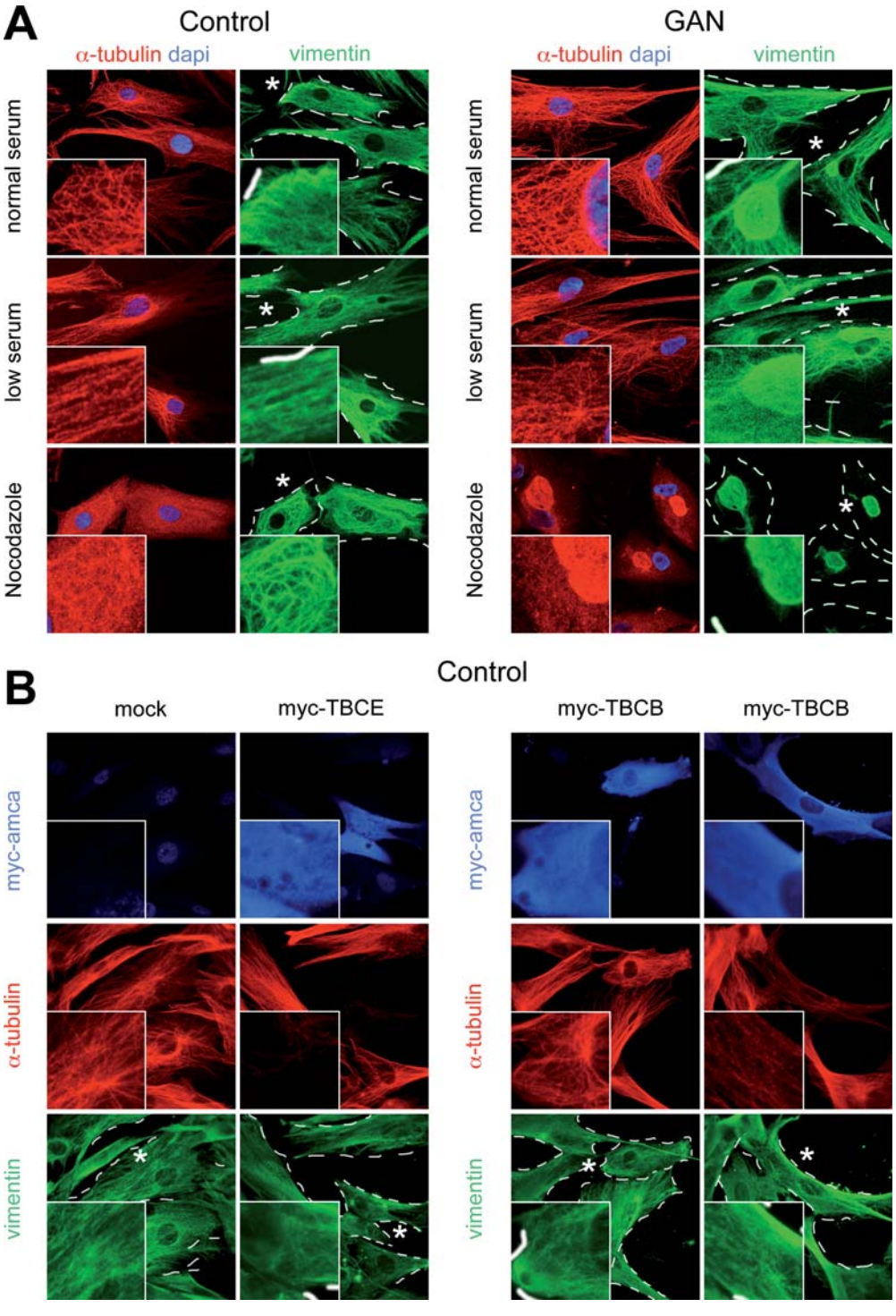

Figure 6. Prolonged microtubule loss does not generate GAN-like aggregates of vimentin in control fibroblasts. The effect of microtubule depolymerization on vimentin distribution was monitored over a 72 h period after (**A**) addition of 10 μM nocodazole and (**B**) overexpression of TBCE (left panel) and TBCB (right panel) on control fibroblasts. The resulting reorganization of vimentin network was compared with (A) (right panel) the characteristic aggregates generated in GAN fibroblasts in normal serum, low serum conditions and after the addition of nocodazole (dense ovoid staining with tubulin results from bleaching from the bright vimentin aggregates). Experiments were conducted three times. Note that the dashed lines (obtained from a merge picture with brightfield) delineate the cellular outline, and the stars represent the region selected for higher magnification.

$GAN^{\Delta 3-5;\Delta 3-5}$ mouse (34) may reflect altered microtubule organization and distribution rather than reduced overall axonal microtubule content. Moreover, since prolonged disassembly of microtubules did not generate the GAN-like ovoid aggregates of vimentin in healthy fibroblasts, the sum of these analyses suggests that IFs aggregation in GAN

patients may not involve TBCB-mediated microtubule disassembly.

MATERIALS AND METHODS

Production of monoclonal antibodies against gigaxonin

Full-length gigaxonin (position 1–1794) and N-terminal part of gigaxonin (position 1–670 with additional TAA) were subcloned in the pRSET-A vector at *Bam*HI site. The corresponding 6× His-tagged full-length and 6× His-tagged Gig^{NH2} gigaxonin proteins, expressed in BL21 *Escherichia coli* after IPTG induction, were solubilized in 8 M urea solution, purified using NiNTA agarose (Qiagen) and eluted in decreasing pH solutions in the continued presence of urea. Antigens were then subsequently recovered from the solution (for the 6× His-Gig^{NH2}) or from an SDS gel (for the 6× His-full-length gigaxonin) using dialysis and electroelution, respectively, and concentrated by Centricon filter centrifugation. Monoclonal antibodies were generated from these immunogens by the Ludwig Institute monoclonal antibody facility. From a total of 35 antibodies generated, two were selected: GigA (from 6× His-tagged Gig^{NH2} antigen) and GigB (from 6× His-tagged full-length antigen) as the most monospecific and sensitive to detect the endogenous gigaxonin by immunoblotting.

Immunoblotting

Protein extracts were prepared from cells after incubation in lysis solution (50 mM Tris pH 7.5; 150 mM NaCl; 1% Triton X-100; 5 mM EDTA and cocktail of proteases inhibitors). Tissues were homogenized in 5:1 (v/w) of solution (150 mM NaCl; 50 mM Tris pH 7.5; 0.1 mM DTT, 1/1000 aprotinin-LPC and 1 mM PMSF), proteins were extracted in the presence of 1% Triton X-100, 1% sodium deoxycholate and 0.1% SDS. A total of 80–100 μg proteins were separated on 8 or 10% SDS–polyacrylamide gels and transferred onto nitrocellulose membranes. The membranes were incubated at room temperature for 1 h in blocking solution [5% non-fat milk in PBST (PBS with 0.05% Tween 20)], at 4°C overnight in primary antibody prepared in blocking solution, washed in PBST and incubated at room temperature for 1 h in secondary antibody in blocking solution. Primary monoclonal antibodies: mouse anti-gigaxonin GigA and GigB (1:150), Flag (M2, Sigma, 1:5000), TBCB (Abnova CKAP1, 1:250) followed by secondary antibodies (sheep anti-mouse IgG, horseradish peroxidase-linked whole antibody from GE Healthcare) were all visualized using SuperSignal West Femto substrate (Pierce). For the detection of internal controls, mouse primary antibodies (DM1α for α-tubulin 1: 10 000, β-actin from Abcam 1:1000 and GAPDH from Ambion 1:4000) were incubated at 4°C overnight in blocking solution complemented with 0.1% sodium azide and revealed using regular ECL substrate (Pierce).

Immunocytochemistry

After expansion in DMEM with 10% serum (or 0.1% serum for fibroblasts when specified) supplemented with 1% penicillin/streptomycin, cells were prepared for immunocytochemistry as follows. After fixation in 4% paraformaldehyde in PBS, cells were incubated in blocking solution (0.1 M glycine; 2.5% fetal bovine serum and 0.1% Triton X-100 in PBS), then with the primary antibodies diluted in the same solution. Washes in PBS/0.1% Triton X-100 were followed by incubation with the secondary antibodies prepared in the blocking solution. All incubations were performed at room temperature for 1 h. The preparations were counterstained with DAPI for 1 min (unless otherwise specified), washed with PBS and coverslips were mounted with an antifading solution (Vectashield, Vector laboratories). Primary antibodies: vimentin (mouse clone V9, Chemicon 1:400); α-tubulin (rat, 1:2000); myc (rabbit, Fitzerald 1:500) and flag (M2-FITC, Sigma 1:100). Secondary antibodies (donkey anti-rabbit AMCA, donkey anti-mouse FITC, donkey anti-rat TR and donkey anti-mouse Cy5) were purchased from Jackson Immunoresearch Laboratories. All images correspond to a composite of Z series taken with a Zeiss confocal microscope. Microtubule depolymerization was achieved by the addition of 10 μM nocodazole to culture media.

Transfection

Myc-TBCB and myc-TBCE constructs were obtained by subcloning TBCB/E cDNA from the original plasmids (generous gift from Dr Nicholas Cowan) in a pcDNA3.1+ vector modified to contain a Kozak-ATG-myc fragment. Gigaxonin mutant clones were derived from the pTL10SFlag-gigaxonin (14) using sequential PCRs. Transfection of Cos cells and human primary fibroblasts were performed using Effectene (Qiagen), and Lipofectamine LTX and PLUS reagents (Invitrogen), respectively.

ACKNOWLEDGEMENTS

The authors wish to thank the Cleveland group and the INMED for their support, particularly Lars Jansen and François Michel for helping on primary fibroblasts expansion and confocal microscopy. The authors are very grateful to Dr Cowan for providing the TBCB/E constructs.

Conflict of Interest Statement. None declared.

FUNDING

This work was supported by the National Institutes of Health (GM27036 to D.W.C); MEXT of Japan, Health and Labour Science Research (K.Y.); Institut National de la Santé et de la Recherche Médicale (INSERM), Association Française contre les Myopathies (AFM 12758) to P.B. Salary support for D.W.C. and P.B is provided by the Ludwig Institute for Cancer Research and INSERM, respectively.

REFERENCES

1. Asbury, A.K., Gale, M.K., Cox, S.C., Baringer, J.R. and Berg, B.O. (1972) Giant axonal neuropathy, a unique case with segmental neurofilamentous masses. *Acta Neuropathol.*, **20**, 237–247.

2. Ben Hamida, C., Cavalier, L., Belal, S., Sanhaji, H., Nadal, N., Barhoumi, C., MRissa, N., Marzouki, N., Mandel, J.L., Ben Hamida, M. *et al.* (1997) Homozygosity mapping of giant axonal neuropathy gene to chromosome 16q24.1. *Neurogenetics*, **1**, 129–133.
3. Berg, B.O., Rosenberg, S.H. and Asbury, A.K. (1972) Giant axonal neuropathy. *Pediatrics*, **49**, 894–899.
4. Bomont, P., Cavalier, L., Blondeau, F., Ben Hamida, C., Belal, S., Tazir, M., Demir, E., Topaloglu, H., Korinthenberg, R., Tuysuz, B. *et al.* (2000) The gene encoding gigaxonin, a new member of the cytoskeletal BTB/Kelch repeat family, is mutated in giant axonal neuropathy. *Nat. Genet.*, **26**, 370–374.
5. Igisu, H., Ohta, M., Tabira, T., Hosokawa, S. and Goto, I. (1975) Giant axonal neuropathy. A clinical entity affecting the central as well as the peripheral nervous system. *Neurology*, **25**, 717–721.
6. Ouvrier, R.A., Prineas, J., Walsh, J.C., Reye, R.D. and McLeod, J.G. (1974) Giant axonal neuropathy, a third case. *Proc. Aust. Assoc. Neurol.*, **11**, 137–144.
7. Koch, T., Schultz, P., Williams, R. and Lampert, P. (1977) Giant axonal neuropathy, a childhood disorder of microfilaments. *Ann. Neurol.*, **1**, 438–451.
8. Peiffer, J., Schlote, W., Bischoff, A., Boltshauser, E. and Muller, G. (1977) Generalized giant axonal neuropathy, a filament-forming disease of neuronal, endothelial, glial, and schwann cells in a patient without kinky hair. *Acta Neuropathol.*, **40**, 213–218.
9. Azzedine, H., Ravise, N., Verny, C., Gabreels-Festen, A., Lammens, M., Grid, D., Vallat, J.M., Durosier, G., Senderek, J., Nouioua, S. *et al.* (2006) Spine deformities in Charcot–Marie–Tooth 4C caused by SH3TC2 gene mutations. *Neurology*, **67**, 602–606.
10. Fabrizi, G.M., Cavallaro, T., Angiari, C., Bertolasi, L., Cabrini, I., Ferrarini, M. and Rizzuto, N. (2004) Giant axon and neurofilament accumulation in Charcot–Marie–Tooth disease type 2E. *Neurology*, **62**, 1429–1431.
11. Fabrizi, G.M., Cavallaro, T., Angiari, C., Cabrini, I., Taioli, F., Malerba, G., Bertolasi, L. and Rizzuto, N. (2007) Charcot–Marie–Tooth disease type 2E, a disorder of the cytoskeleton. *Brain*, **130**, 394–403.
12. Lus, G., Nelis, E., Jordanova, A., Lofgren, A., Cavallaro, T., Ammendola, A., Melone, M.A., Rizzuto, N., Timmerman, V., Cotrufo, R. *et al.* (2003) Charcot–Marie–Tooth disease with giant axons, a clinicopathological and genetic entity. *Neurology*, **61**, 988–990.
13. Lariviere, R.C. and Julien, J.P. (2004) Functions of intermediate filaments in neuronal development and disease. *J. Neurobiol.*, **58**, 131–148.
14. Bomont, P. and Koenig, M. (2003) Intermediate filament aggregation in fibroblasts of giant axonal neuropathy patients is aggravated in non dividing cells and by microtubule destabilization. *Hum. Mol. Genet.*, **12**, 813–822.
15. Prineas, J.W., Ouvrier, R.A., Wright, R.G., Walsh, J.C. and McLeod, J.G. (1976) Giant axonal neuropathy, a generalized disorder of cytoplasmic microfilament formation. *J. Neuropathol. Exp. Neurol.*, **35**, 458–470.
16. Klymkowsky, M.W. and Plummer, D.J. (1985) Giant axonal neuropathy, a conditional mutation affecting cytoskeletal organization. *J. Cell Biol.*, **100**, 245–250.
17. Pena, S.D. (1981) Giant axonal neuropathy, intermediate filament aggregates in cultured skin fibroblasts. *Neurology*, **31**, 1470–1473.
18. Pena, S.D., Opas, M., Turksen, K., Kalnins, V.I. and Carpenter, S. (1983) Immunocytochemical studies of intermediate filament aggregates and their relationship to microtubules in cultured skin fibroblasts from patients with giant axonal neuropathy. *Eur. J. Cell Biol.*, **31**, 227–234.
19. Bomont, P., Ioos, C., Yalcinkaya, C., Korinthenberg, R., Vallat, J.M., Assami, S., Munnich, A., Chabrol, B., Kurlemann, G., Tazir, M. *et al.* (2003) Identification of seven novel mutations in the GAN gene. *Hum. Mutat.*, **21**, 446–451.
20. Bruno, C., Bertini, E., Federico, A., Tonoli, E., Lispi, M.L., Cassandrini, D., Pedemonte, M., Santorelli, F.M., Filocamo, M., Dotti, M.T. *et al.* (2004) Clinical and molecular findings in patients with giant axonal neuropathy (GAN). *Neurology*, **62**, 13–16.
21. Demir, E., Bomont, P., Erdem, S., Cavalier, L., Demirci, M., Kose, G., Muftuoglu, S., Cakar, A.N., Tan, E., Aysun, S. *et al.* (2005) Giant axonal neuropathy: clinical and genetic study in six cases. *J. Neurol. Neurosurg. Psychiatr.*, **76**, 825–832.
22. Houlden, H., Groves, M., Miedzybrodzka, Z., Roper, H., Willis, T., Winer, J., Cole, G. and Reilly, M.M. (2007) New mutations, genotype phenotype studies and manifesting carriers in giant axonal neuropathy. *J. Neurol. Neurosurg. Psychiatr.*, **78**, 1267–1270.
23. Koop, O., Schirmacher, A., Nelis, E., Timmerman, V., De Jonghe, P., Ringelstein, B., Rasic, V.M., Evrard, P., Gärtner, J., Claeys, K.G. *et al.* (2007) Genotype–phenotype analysis in patients with giant axonal neuropathy. *Neuromuscul. Disord.*, **17**, 624–630.
24. Kuhlenbaumer, G., Young, P., Oberwittler, C., Hunermund, G., Schirmacher, A., Domschke, K., Ringelstein, B. and Stogbauer, F. (2002) Giant axonal neuropathy (GAN), case report and two novel mutations in the gigaxonin gene. *Neurology*, **58**, 1273–1276.
25. Leung, C.L., Pang, Y., Shu, C., Goryunov, D. and Liem, R.K. (2007) Alterations in lipid metabolism gene expression and abnormal lipid accumulation in fibroblast explants from giant axonal neuropathy patients. *BMC Genet.*, **8**, 6–10.
26. Nalini, A., Gayathri, N., Yasha, T.C., Ravishankar, S., Urtizberea, A., Huehne, K. and Rautenstrauss, B. (2008) Clinical, pathological and molecular findings in two siblings with giant axonal neuropathy (GAN), report from India. *Eur. J. Med. Genet.*, **51**, 426–435.
27. McClellan, A.J., Tam, S., Kaganovich, D. and Frydman, J. (2005) Protein quality control, chaperones culling corrupt conformations. *Nat. Cell Biol.*, **7**, 736–741.
28. Kitada, T., Asakawa, S., Hattori, N., Matsumine, H., Yamamura, Y., Minoshima, S., Yokochi, M., Mizuno, Y. and Shimizu, N. (1998) Mutations in the parkin gene cause autosomal recessive juvenile parkinsonism. *Nature*, **9**, 605–608.
29. Furukawa, M., He, Y.J., Borchers, C. and Xiong, Y. (2003) Targeting of protein ubiquitination by BTB-Cullin 3-Roc1 ubiquitin ligases. *Nat. Cell Biol.*, **5**, 1001–1007.
30. Pintard, L., Willis, J.H., Willems, A., Johnson, J.L., Srayko, M., Kurz, T., Glaser, S., Mains, P.E., Tyers, M., Bowerman, B. *et al.* (2003) The BTB protein MEL-26 is a substrate-specific adaptor of the CUL-3 ubiquitin-ligase. *Nature*, **425**, 311–316.
31. Xu, L., Wei, Y., Reboul, J., Vaglio, P., Shin, T.H., Vidal, M., Elledge, S.J. and Harper, J.W. (2003) BTB proteins are substrate-specific adaptors in an SCF-like modular ubiquitin ligase containing CUL-3. *Nature*, **425**, 316–321.
32. Allen, E., Ding, J., Wang, W., Pramanik, S., Chou, J., Yau, V. and Yang, Y. (2005) Gigaxonin-controlled degradation of MAP1B light chain is critical to neuronal survival. *Nature*, **438**, 224–228.
33. Ding, J., Allen, E., Wang, W., Valle, A., Wu, C., Nardine, T., Cui, B., Yi, J., Taylor, A., Jeon, N.L. *et al.* (2006) Gene targeting of GAN in mouse causes a toxic accumulation of microtubule-associated protein 8 and impaired retrograde axonal transport. *Hum. Mol. Genet.*, **15**, 1451–1463.
34. Wang, W., Ding, J., Allen, E., Zhu, P., Zhang, L., Vogel, H. and Yang, Y. (2005) Gigaxonin interacts with tubulin folding cofactor B and controls its degradation through the ubiquitin-proteasome pathway. *Curr. Biol.*, **15**, 2050–2055.
35. Ding, J., Liu, J.J., Kowal, A.S., Nardine, T., Bhattacharya, P., Lee, A. and Yang, Y. (2002) Microtubule-associated protein 1B, a neuronal binding partner for gigaxonin. *J. Cell Biol.*, **158**, 427–433.
36. Kortazar, D., Fanarraga, M.L., Carranza, G., Bellido, J., Villegas, J.C., Avila, J. and Zabala, J.C. (2007) Role of cofactors B (TBCB) and E (TBCE) in tubulin heterodimer dissociation. *Exp. Cell Res.*, **313**, 425–436.
37. Dequen, F., Bomont, P., Gowing, G., Cleveland, D.W. and Julien, J.P. (2008) Modest loss of peripheral axons, muscle atrophy and formation of brain inclusions in mice with targeted deletion of gigaxonin exon 1. *J. Neurochem.*, **107**, 253–264.
38. Gurland, G. and Gundersen, G.G. (1995) Stable, detyrosinated microtubules function to localize vimentin intermediate filaments in fibroblasts. *J. Cell Biol.*, **131**, 1275–1290.
39. Gyoeva, F.K. and Gelfand, V.I. (1991) Coalignment of vimentin intermediate filaments with microtubules depends on kinesin. *Nature*, **353**, 445–448.
40. Ho, C.L., Martys, J.L., Mikhailov, A., Gundersen, G.G. and Liem, R.K. (1998) Novel features of intermediate filament dynamics revealed by green fluorescent protein chimeras. *J. Cell Sci.*, **111**, 1767–1778.
41. Klymkowski, M. (1981) Intermediate filaments in 3T3 cells collapse after intracellular injection of a monoclonal anti-intermediate filament antibody. *Nature*, **249**, 249–251.
42. Kreitzer, G., Liao, G. and Gundersen, G.G. (1999) Detyrosination of tubulin regulates the interaction of intermediate filaments with microtubules *in vivo* via a kinesin dependent mechanism. *Mol. Biol. Cell*, **10**, 1105–1118.

43. Roy, S. (1993) Role of stress fibers in the association of intermediate filaments with microtubules in fibroblasts cells. *Cell Biol. Int.*, **17**, 645–652.
44. Yoon, M., Moir, R.D., Prahlad, V. and Goldman, R.D. (1998) Motile properties of vimentin intermediate filament networks in living cells. *J. Cell Biol.*, **143**, 147–157.
45. Bhamidipati, A., Lewis, S.A. and Cowan, N.J. (2000) ADP ribosylation factor-like protein 2 (Arl2) regulates the interaction of tubulin-folding cofactor D with native tubulin. *J. Cell Biol.*, **149**, 1087–1096.
46. Tian, G., Lewis, S.A., Feierbach, B., Stearns, T., Rommelaere, H., Ampe, C. and Cowan, N.J. (1997) Tubulin subunits exist in an activated conformational state generated and maintained by protein cofactors. *J. Cell Biol.*, **138**, 821–832.
47. Cullen, V.C., Brownlees, J., Banner, S., Anderton, B.H., Leigh, P.N., Shaw, C.E. and Miller, C.C. (2004) Gigaxonin is associated with the Golgi and dimerises via its BTB domain. *Neuroreport*, **15**, 873–876.
48. Donaghy, M., King, R.H., Thomas, P.K. and Workman, J.M. (1988) Abnormalities of the axonal cytoskeleton in giant axonal neuropathy. *J. Neurocytol.*, **17**, 197–208.
49. Treiber-Held, S., Budjarjo-Welim, H., Reimann, D., Richter, J., Kretzschmar, H.A. and Hanefeld, F. (1994) Giant axonal neuropathy, a generalized disorder of intermediate filaments with longitudinal grooves in the hair. *Neuropediatrics*, **25**, 89–93.
50. Tian, G., Huang, Y., Rommelaere, H., Vandekerckhove, J., Ampe, C. and Cowan, N.J. (1996) Pathway leading to correctly folded beta tubulin. *Cell*, **86**, 287–296.
51. Bartolini, F., Tian, G., Piehl, M., Cassimeris, L., Lewis, S.A. and Cowan, N.J. (2005) Identification of a novel tubulin destabilizing protein related to the chaperone cofactor E. *J. Cell Sci.*, **118**, 1197–1207.
52. Martin, L., Fanarraga, M.L., Aloria, K. and Zabala, J.C. (2000) Tubulin folding cofactor D is a microtubule destabilizing protein. *FEBS Lett.*, **470**, 93–95.